Available online at www.sciencedirect.com
SCIENCE DIRECT®
ELSEVIER
Journal of Magnetic Resonance 170 (2004) 149–155
JMR Journal of Magnetic Resonance
www.elsevier.com/locate/jmr

Communication

Design of a capacitively decoupled transmit/receive NMR phased array for high field microscopy at 14.1 T

Xiaozhong Zhang and Andrew Webb*

Department of Electrical and Computer Engineering, Beckman Institute for Advanced Science and Technology, University of Illinois at Urbana-Champaign, Urbana, IL 61801, USA
Physikalisches Institut, University of Würzburg, Germany

Received 17 February 2004; revised 29 April 2004
Available online 10 July 2004

Abstract

A design is presented for a "phased array" of four transmit/receive saddle-geometry volume coils for microimaging at 600 MHz within a 45 mm clear-bore vertical magnet. The small size of the coils, ~10 mm in length, and high frequency of operation both present considerable challenges for the design of a phased array. The particular design consists of four saddle coils, stacked vertically, in order to produce an array suitable for imaging samples, typical of many microimaging studies, with a large length:diameter ratio. Optimal coil overlap is used to reduce the mutual inductance between adjacent coils, and capacitive networks are used to maximize the isolation between all of the coils. Standard 50 Ω input impedance preamplifiers are used so that the preamplifiers do not have to be integrated directly into the probe. Isolation between coils was better than 20 dB for all coil pairs. An increase in signal-to-noise of $70 \pm 3\%$ was achieved, averaged over the whole array, compared to a single coil of the same dimensions. High resolution phased array images are shown for ex vivo tissue samples.

1. Introduction

The use of mutually decoupled coil arrays [1,2], often termed phased arrays, in magnetic resonance imaging has become widespread, both in applications where increased sensitivity over a large field-of-view is required, and in cases where partially parallel imaging techniques can be used to speed up data acquisition by utilizing the inherent spatial information of the coils [3–5]. A variety of phased-array coil designs have been constructed [6–13], usually for clinical applications at field strengths below 4 T. In any design, each individual coil in the array needs to be electrically isolated from the others to minimize the correlated noise [1,2,14]. Coil coupling is determined by the mutual impedance between coils and the relative magnitude of the currents in the coils. Coil overlap can be used to reduce the mutual impedance, and the use of high input impedance amplifiers [1] with appropriate matching networks [1,15] reduces the currents in the coils. Cable traps [16,17] are also commonly used for reducing coupling between the cables feeding each element of the array. Other methods for decreasing the effective coil coupling include capacitive networks [18–21], negative mutual inductance [22] and $2n$-port networks [23]. In most cases, the individual coils of the array are receive only, and a volume coil is used for homogeneous transmission, although some versions of transmit/receive phased arrays have been published recently [24–26].

The design of phased array coils for high-field NMR microscopy has received relatively little attention despite the possibilities of increasing the signal-to-noise ratio (SNR), which generally limits the attainable spatial resolution, or decreasing the typically long data acquisition times. There are a number of issues which arise in the implementation of such array coils. In addition to the intrinsic problems associated with coil design at high frequencies, where the coil dimensions can be a considerable fraction of the radiofrequency (RF) wavelength, limited space within vertical bore magnets makes it difficult to incorporate both transmit and receive coils.

* Corresponding author. Fax: 1-217-244-0105.
E-mail address: agwebb@uiuc.edu (A. Webb).

1090-7807/$ - see front matter © 2004 Published by Elsevier Inc.
doi:10.1016/j.jmr.2004.05.004

In addition, it is often desirable to have a homogeneous reception field such that the entire sample, rather than just the surface can be imaged. At high frequencies it becomes increasingly difficult to reduce the currents in the coils by using low- or high-input impedance preamplifiers. If such preamplifiers are to be used, they must also be placed very close to the coils (in order to minimize line loss due to impedance mismatches), which is difficult to implement given the limited space available. Two papers have been published which have showed the feasibility of phased-array imaging at a proton frequency of 200 MHz [27,28], although these were implemented with a wide-bore horizontal magnet. These designs used array loops with dimensions approximately 3.8×5 cm. Since the clear bore within the gradients of our 600 MHz vertical-bore magnet is 4.5 cm, we have to reduce considerably the dimensions of the individual elements of the array.

To this end, we have designed a probehead incorporating four transmit/receive saddle-geometry [29] volume coils. Since many of our microimaging studies of ex vivo biological tissue, e.g., spinal cords, plant specimens, and separation columns, use samples with a high length-to-diameter ratio, the particular design consists of four saddle coils, stacked vertically. Standard 50 Ω input preamplifiers are used such that the preamplifiers do not have to be integrated directly into the probe. In addition to reducing mutual inductance between adjacent elements of the array by optimal coil overlap, capacitive networks are used for increased coil isolation between all of the coils. The array has been designed for imaging tissue samples at 600 MHz within a 45 mm clear-bore magnet, using a console with four receiver channels.

2. Capacitive decoupling networks

Fig. 1A shows a circuit model of a balanced impedance-matched coil. In this figure the coil is effectively split into two halves, with L_1 representing one-quarter of the total self-inductance of the coil, and R_1 one-half of the total resistance. Since the two "inductors" L_1 are highly coupled due to their close proximity, the coupling coefficient is approximately equal to unity. The mutual inductance, M_1, is given by

$$M_1 \approx \sqrt{L_1 \times L_1} \approx L_1. \tag{1}$$

Simple simulations (Advanced Design Software, Agilent, Palo Alto) show that the voltage at the center of the coil approaches zero as the loss of the coil is reduced, and that for a sample coil with a fairly high loaded Q value, e.g., about 150 for the coils used in this probe design, the RF voltage at the center of the coil is very small compared with that across the whole coil. It is convenient to consider the RF voltage at the coil center to be zero, such that vector analysis for crosstalk can be simplified.

The circuit model of a pair of balanced impedance matched coils is shown in Fig. 1B, omitting the tuning

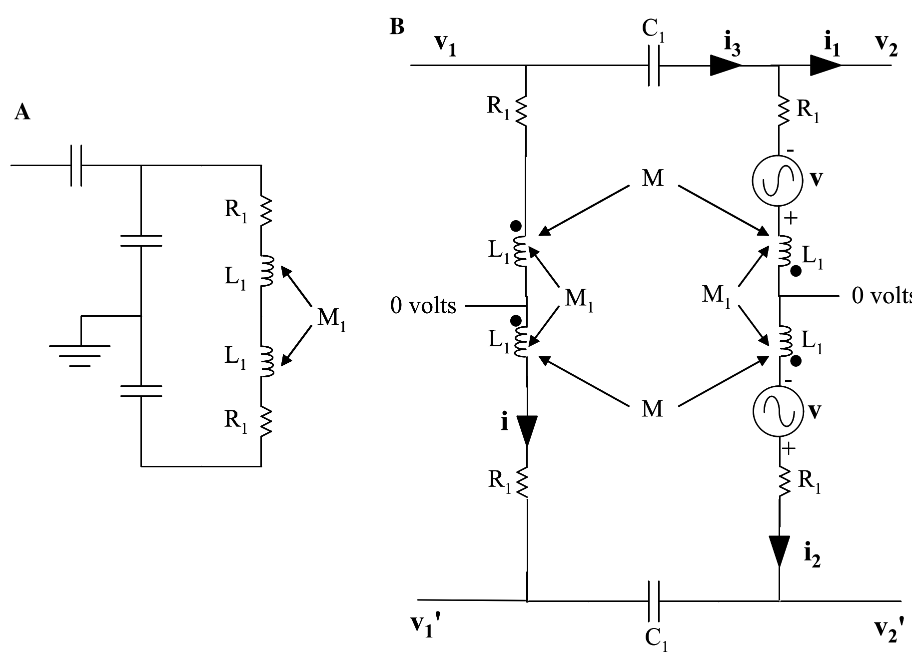

Fig. 1. (A) A circuit model of a balanced impedance matched coil. $L_1 = L_{coil}/4$, $R_1 = R_{coil}/2$. Since the coupling between the two halves of the coil is strong, the value of the mutual inductance between the two, M_1, is approximately equal to L_1. (B) A circuit model of a pair of balanced-matched coils, omitting the impedance matching networks, to simulate the S_{21}, i.e., the response of coil 2 on the right to a stimulus from coil 1 on the left. The voltage source $\boldsymbol{v}$ represents the induced voltage across the inductors L_1 due to the mutual inductance M between the two coils (note that the value of M is negative in this configuration). C_1 represents the parasitic capacitance between the two coils.

and matching network, with the primary coil on the left. The voltages $\boldsymbol{v}_1$, $\boldsymbol{v}_2$, $\boldsymbol{v}'_1$, and $\boldsymbol{v}'_2$ are those at the terminals of the primary and secondary coils, with respect to virtual ground at the center of the coils, and $\boldsymbol{v}$ represents the voltage induced in the secondary coil from current in the primary coil. Assuming that the current $\boldsymbol{i}$ has zero phase, and setting $\boldsymbol{v}_2$ to zero, the voltage $\boldsymbol{v}_1$ is given by:

$$\begin{aligned}\boldsymbol{v}_1 &= \boldsymbol{i}(R_1 + \mathrm{j}\omega(L_1 + M_1)) \\ &= |\boldsymbol{i}(R_1 + \mathrm{j}2\omega L_1)|\angle(90^\circ - \theta),\end{aligned} \tag{2}$$

where θ is the loss angle of the loaded sample coil, i.e.,

$$\theta = \tan^{-1}\frac{1}{Q_{\text{loaded}}} = \tan^{-1}\frac{R_1}{2\omega L_1}. \tag{3}$$

Due to circuit symmetry

$$\boldsymbol{v}'_1 = -\boldsymbol{v}_1 = |\boldsymbol{i}(R_1 + \mathrm{j}2\omega L_1)|\angle(-90^\circ - \theta). \tag{4}$$

The induced voltages on the right-hand-side of the circuit are given by:

$$\boldsymbol{v} = \mathrm{j}\omega M \quad \boldsymbol{i} = |\omega M \boldsymbol{i}|\angle 90^\circ. \tag{5}$$

The current in the secondary coil is:

$$\boldsymbol{i}_2 = \frac{\boldsymbol{v}}{R_1 + \mathrm{j}\omega(L_1 + M_1)} = \left|\frac{\boldsymbol{v}}{R_1 + \mathrm{j}2\omega L_1}\right|\angle\theta. \tag{6}$$

The current $\boldsymbol{i}_3$ is given by:

$$\boldsymbol{i}_3 = \frac{\boldsymbol{v}_1 - \boldsymbol{v}_2}{R_c + \frac{1}{\mathrm{j}\omega C_1}} = \left|\frac{\boldsymbol{v}_1}{R_c + \frac{1}{\mathrm{j}\omega C_1}}\right|\angle(180^\circ - \theta - \gamma), \tag{7}$$

where R_c is the loss resistance of the capacitor C_1, and γ is the loss angle of C_1, i.e.,

$$\gamma = \tan^{-1}\frac{1}{Q_{\text{capacitor}}} = \tan^{-1} R_c\omega C_1. \tag{8}$$

The total crosstalk current $\boldsymbol{i}_1$, as shown in Fig. 1B, is given by:

$$\boldsymbol{i}_1 = \boldsymbol{i}_3 - \boldsymbol{i}_2. \tag{9}$$

One possibility to decouple the two coils is to use an LC circuit to invert the direction of $\boldsymbol{i}_3$ [30]. However, inductors, which have to be wound from thin wire due to space considerations, typically have relatively low Q values at 600 MHz. The RF voltage $\boldsymbol{v}'_1$ can also be used to provide a current that has a 180° phase difference with respect to $\boldsymbol{i}_3$. Since $\boldsymbol{v}_1$ and $\boldsymbol{v}'_1$ are 180° out of phase, connecting a capacitor between the points at $\boldsymbol{v}'_1$ and $\boldsymbol{v}_2$ is equivalent to connecting an inductor between the points at $\boldsymbol{v}_1$ and $\boldsymbol{v}_2$, as follows. Connecting the inductor L would introduce an additional current, $\boldsymbol{i}_L = \boldsymbol{v}_1/j\omega L$. Conversely, adding a capacitor C introduces an extra current, $\boldsymbol{i}_C = -v_1/j\omega C$. These currents are identical under the condition $C = (\omega^2 L)^{-1}$. A variable capacitor C_d, as shown in Fig. 2A can therefore be used for decoupling the coil pair. Since capacitors normally have much higher quality factors than inductors at 600 MHz, images with higher SNR are expected from using capacitors as decoupling components. The capacitor C_d is shown with a loss angle β, i.e.,

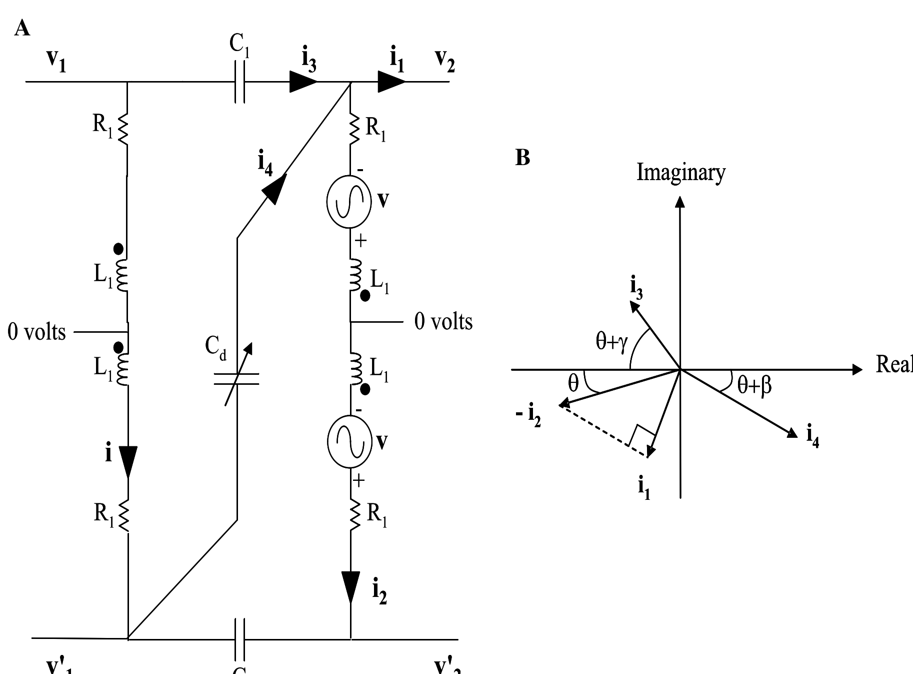

Fig. 2. (A) A variable capacitor C_d can be used to decouple non-adjacent coils. (B) Diagram showing a vector analysis of the coil cross-talk. The angles θ, γ, and β are defined in Eqs. (3), (8), and (10). The current introduced by C_d is necessary for minimizing the magnitude of $\boldsymbol{i}_1$ by compensating for $\boldsymbol{i}_3$.

$$\beta = \tan^{-1}\frac{1}{Q_{\text{capacitor}}} = \tan^{-1} R_{\text{d}}\omega C_{\text{d}}, \tag{10}$$

where R_{d} is the loss resistance of capacitor C_{d}. Fig. 2B shows a vector analysis of the cross-talk current. Since the loss angles cannot be altered, the value of the variable capacitor C_{d} is adjusted such that $\boldsymbol{i}_1$ is perpendicular to the vector sum of $\boldsymbol{i}_3$ and $\boldsymbol{i}_4$, which corresponds to the minimum cross-talk achievable, since:

$$\boldsymbol{i}_1 = \boldsymbol{i}_3 + \boldsymbol{i}_4 - \boldsymbol{i}_2. \tag{11}$$

3. Experimental setup

All experiments were performed at 600 MHz using a Varian Unity console with four identical receiver channels. The clear bore inside the gradient set is 45 mm. Each saddle coil was 10 mm in length, 8 mm in diameter and constructed from 26 AWG copper wire (California Fine Wire, Grover Beach, CA). An overlap of 1 mm was used between each coil, resulting in a total length of the array of 37 mm: this value was chosen to fit within the linear region of the magnetic field gradients. The inductance of each coil was ~63 nH, the total distributed capacitance was 0.466 pF with no load, giving a self-resonance frequency ~930 MHz. The full decoupling network is shown in Fig. 3. Photographs of the coil assembly are shown in Fig. 4. Samples were placed in an 8 mm NMR tube. Standard spin-echo and gradient-echo two-dimensional multislice and three-dimensional sequences were run. A four-way power-splitter (Minicircuits) was used on the transmit side of the probe.

4. Results

Table 1 shows the degree of isolation between adjacent and non-adjacent coils: in all cases the isolation was greater than 20 dB. Fig. 5 shows the projections obtained from each coil using a water phantom. A spin-echo projection sequence was used with no slice selection, an echo time of 20 ms, and the frequency encoding gradient applied along the axial (z) dimension. The coil-to-coil signal bleedthrough in all cases is well below 10%, consistent with the electrical isolation being greater than 20 dB. The axial coil profiles are also consistent with those expected for individual saddle coils.

A signal-to-noise comparison was performed for a sample of 100 mM NaCl solution, using the phased array and a single saddle coil of the same overall dimensions. The single-turn saddle coil was constructed from 26 AWG magnet wire, was 8 mm inner diameter, and 37 mm long. Three fixed capacitors were used to split the conductor into four equal length segements. A standard balanced impedance matching circuit was used. As described by Beck and Blackband [27] the SNR of the array was estimated by measuring the SNR in each

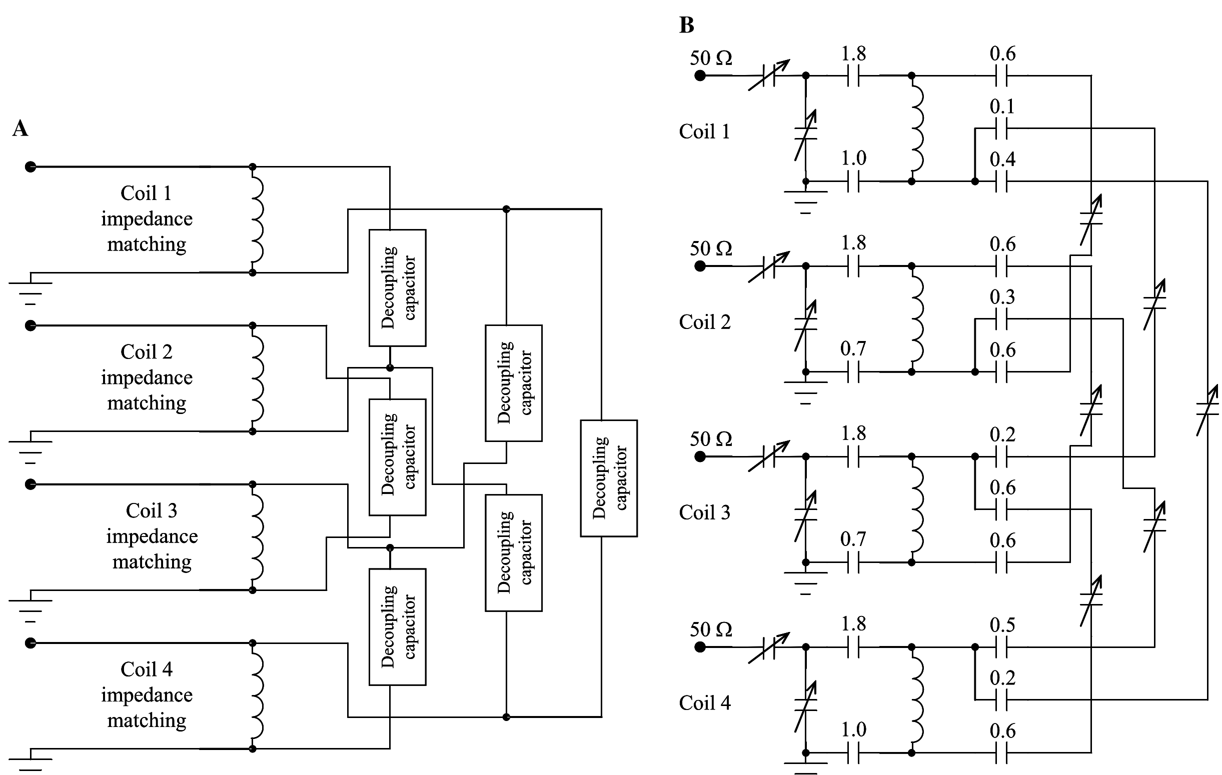

Fig. 3. (A) Block diagram of the probe circuit. (B) Circuit diagram with capacitor values in pF.

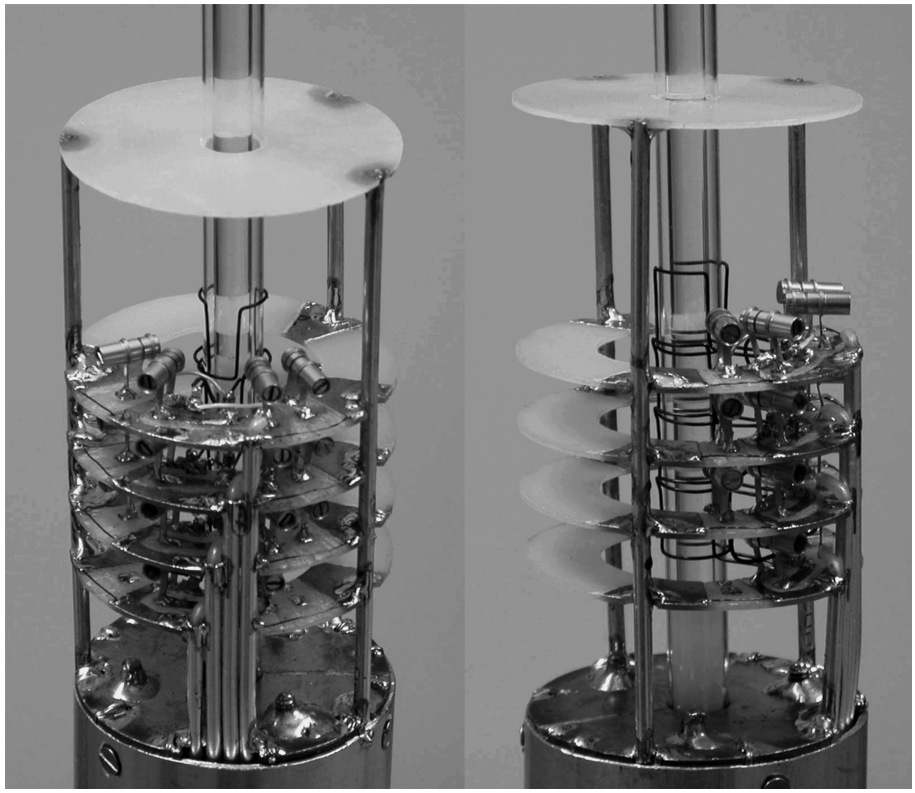

Fig. 4. Photographs of the four-coil probehead, showing the impedance matching and decoupling capacitors. A Faraday shield is placed around the coils in the magnet. A four-way power splitter is used between the transmitter and the individual coils.

Table 1
Coil isolation (dB) at 600 MHz

	Coil 1	Coil 2	Coil 3
Coil 1	xxx		
Coil 2	28.6	xxx	
Coil 3	24.3	22.7	xxx
Coil 4	31.1	42.5	20.1

magnitude image of the array and then calculating the square root of the sum of squares of the individual SNRs. This procedure gives a good estimate of the array SNR, given weak coupling and noise correlation between the individual coils of the array. The SNR for the large saddle coil was measured conventionally by calculating the mean signal intensity divided by the standard deviation of the noise. Since the SNR values are high, typically above 400:1 for the individual array elements, particular care was taken to ensure that the areas selected for noise measurements were free of image artifacts, which can unduly bias the results. Results showed that the SNR was increased by an average of $70 \pm 3\%$ averaged over the entire sample.

Fig. 6 shows images from an ex-vivo tail of *scireus griseus*, which forms part of an on-going project investigating cartilage development in mammals. The in-plane spatial resolution was $75 \times 30\,\mu m$ with a slice thickness of $250\,\mu m$. The combined image is calculated by sum-of-squares, an analysis of which has been published recently [31].

5. Conclusions

This paper has presented a design for a four-coil transmit and receive phased array for magnetic resonance microscopy at 600 MHz. The design is aimed towards samples which have a much greater length than diameter, as is typical for many tissue and plant samples. For this type of sample, the conventional phased array coil designs in which a number of elements are placed around the sample in a "radial" direction is not easily implemented. Instead, we have designed a phased array consisting of multiple volume coils, which are overlapped in the *z*-direction of a vertical bore magnet. Signal-to-noise increases of ~70% over a similarly sized single loop coil were achieved. In the situation, where samples losses are completely dominant, and coil losses can be ignored, the phased array would give an increase in SNR of 100% over a linearly polarized, single, large coil. Since, in most imaging experiments even at high fields, the coil losses cannot be completely discounted, and in our decoupling scheme we have introduced a number of extra components, each of which add some

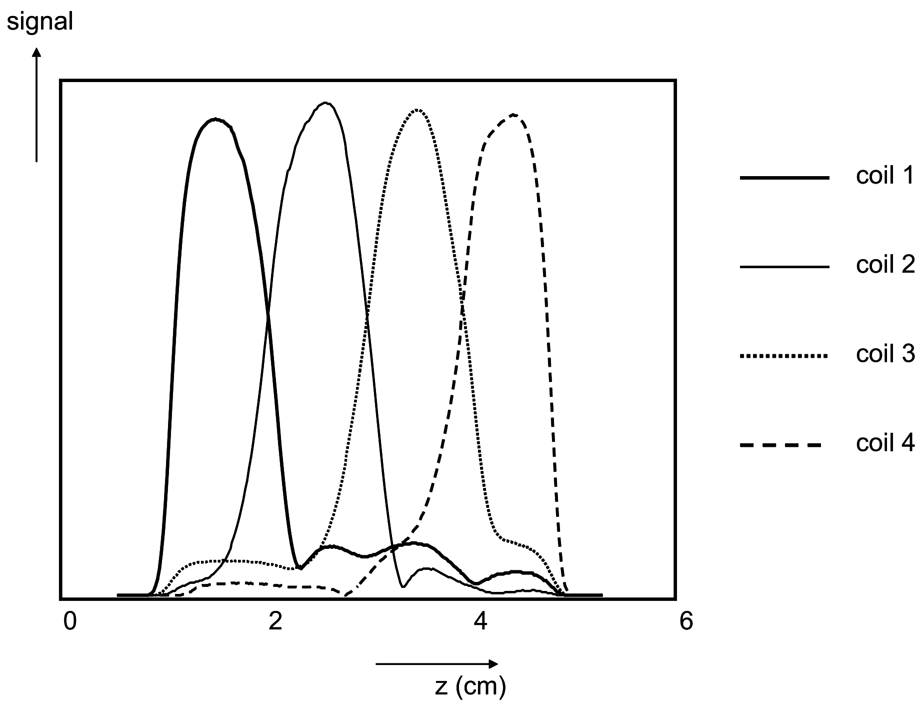

Fig. 5. Spin-echo projections from each of the four receiver coils using a homogenous water phantom of diameter 5 mm and length 60 mm.

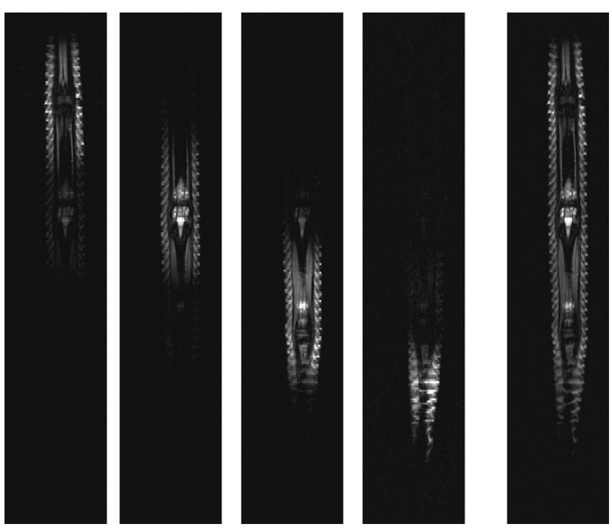

Fig. 6. Images of the tail from *Scirius griseus* obtained from each receiver coil (left) and the combined sum-of-squares image (right). Imaging parameters: field-of-view 40×8 mm, data matrix 512×256, echo time 20 ms, repetition time 1 s, number of averages 2, slice thickness 250 μm, in-plane resolution 75×30 μm.

loss to the probe, the practical SNR is somewhat less than the maximum, but nevertheless significantly above that of the large coil, even were this to have been designed as a circularly polarized coil. For in vivo applications, including the incorporation of partially parallel imaging techniques, we are currently investigating the extension of capacitive decoupling schems to high-field array designs, incorporating both a large transmit and smaller individual receive coils.

Acknowledgments

This project was funded in part by the National Institutes of Health (8RO1EB002343-07), the National Science Foundation with a CAREER award, and the Alexander von Humboldt Foundation under the Wolfgang Paul Programme.

References

[1] P.B. Roemer, W.A. Edelstein, C.E. Hayes, S.P. Souza, O.M. Mueller, The NMR phased array, Magn. Reson. Med. 16 (1990) 192–225.

[2] S.M. Wright, R.L. Magin, J.R. Kelton, Arrays of mutually coupled receiver coils: theory and application, Magn. Reson. Med. 17 (1991) 252–268.

[3] D.K. Sodickson, W.J. Manning, Simultaneous acquisition of spatial harmonics (SMASH): fast imaging with radiofrequency coil arrays, Magn. Reson. Med. 38 (1997) 591–603.

[4] K.P. Pruessman, M. Weiger, M.B. Scheidegger, P. Boesinger, SENSE: sensitivity encoding for fast MRI, Magn. Reson. Med. 42 (1999) 952–962.

[5] M.A. Griswold, P.M. Jakob, R.M. Heidemann, M. Nittka, V. Jellus, J. Wang, B. Kiefer, A. Haase, Generalized autocalibrating partially parallel acquisitions (GRAPPA), Magn. Reson. Med. 47 (2002) 1202–1210.

[6] J.R. Porter, S.M. Wright, A. Reykowski, A 16-element phased-array head coil, Magn. Reson. Med. 40 (1998) 272–279.

[7] J.A. Bankson, M.A. Griswold, S.M. Wright, D.K. Sodickson, SMASH imaging with an eight element multiplexed RF coil array, Magn. Reson. Mater. Phys. Biol. Med. 10 (2000) 93–104.

[8] E.A. Barberi, J.S. Gati, B.K. Rutt, R.S. Menon, A transmit-only/receive-only (TORO) RF system for high-field MRI/MRS applications, Magn. Reson. Med. 43 (2000) 284–289.
[9] P.A. Bottomley, C.H. Lugo Olivieri, R. Giaquinto, What is the optimum phased array coil design for cardiac and torso magnetic resonance?, Magn. Reson. Med. 37 (1997) 591–599.
[10] M. Weiger, K.P. Pruessmann, C. Leussler, R. Roschmann, P. Boesiger, Specific coil design for SENSE: a six-element cardiac array, Magn. Reson. Med. 45 (2001) 495–504.
[11] J.A. de Zwart, P.J. Ledden, P. Kellman, P. van Gelderen, J.H. Duyn, Design of a SENSE-optimized high-sensitivity MRI receive coil for brain imaging, Magn. Reson. Med. 47 (2002) 1218–1227.
[12] D.K. Sodickson, C.A. McKenzie, M.A. Ohliger, E.N. Yeh, M.D. Price, Recent advances in image reconstruction, coil sensitivity calibration, and coil array design for SMASH and generalized parallel MRI, Magn. Reson. Mater. Phys. Biol. Med. 13 (2002) 158–163.
[13] A. Liffers, H.H. Quick, C.U. Herborn, H. Ermert, M.E. Ladd, Geometrical optimization of a phased array coil for high-resolution MR imaging of the carotid arteries, Magn. Reson. Med. 50 (2003) 439–443.
[14] C.E. Hayes, P.B. Roemer, Noise correlations in data simultaneously acquired from multiple surface coil arrays, Magn. Reson. Med. 16 (1990) 181–191.
[15] A. Reykowski, S.M. Wright, J.R. Porter, Design of matching networks for low noise preamplifiers, Magn. Reson. Med. 33 (1995) 848–852.
[16] H. Barfuss, H. Fischer, D. Hentschel, R. Ladebeck, A. Oppelt, R. Wittig, W. Duerr, R. Oppelt, In vivo magnetic resonance imaging and spectroscopy of humans with a 4 T whole-body magnet, NMR Biomed. 3 (1990) 31–45.
[17] D.M. Peterson, B.L. Beck, G.R. Duensing, J. Fitzsimmons, Common mode signal rejection methods for MRI: reduction of cable shield currents for high static magnetic field systems, Magn. Reson. Eng. B 19 (2003) 1–8.
[18] T.R.Fox, Capacitive network to cancel coupling between channels in MRI quadrature antenna, in: Proceedings of the 8th Soc. Magn. Reson., Amsterdam, 1989, p. 99.
[19] J. Wang, A novel method to reduce the signal coupling of surface coils for MRI, in: Proceedings of the 4th International Soc. Magn. Reson. Med., New York, 1996, p. 1434.
[20] J. Lian, P.B. Roemer, MRI RF coil, 1998, US Patent #5,804,969.
[21] J. Jevtic, Ladder networks for capacitive decoupling in phased-array coils, in: Proceedings of the 9th Int. Soc. Magn. Reson. Med., Denver, 2001, p. 17.
[22] T. Nabeshima, T. Takahashi, Y. Matsunaga, E. Yamamoto, K. Katakura, RF probe for MRI, 1996, US Patent #5,489,847.
[23] R.F. Lee, R.O. Giaquinto, C.J. Hardy, Coupling and decoupling theory and its application to the MRI phased array, Magn. Reson. Med. 48 (2002) 203–213.
[24] D.M. Peterson, G.R. Duensing, J. Caserta, J.R. Fitzsimmons, An MR transceive phased array designed for spinal cord imaging at 3 T: preliminary investigations of spinal cord imaging at 3 T, Invest. Radiol. 38 (2003) 428–435.
[25] S. Su, M.X. Zou, J. Murphy-Boesch, Solenoidal array coils, Magn. Reson. Med. 47 (2002) 794–799.
[26] G. Adriany, P. Van de Moortele, F. Wiesinger, X. Zhang, C. Snyder, W. Chen, K. Pruessmann, P. Boesiger, T. Vaughan, K. Ugurbil, Transceive stripline arrays for ultra high field parallel imaging applications, in: Proceedings of the 11th ISMRM, Toronto, Canada, 2003, p. 474.
[27] B.L. Beck, S.J. Blackband, Phased array imaging on a 4.7 T/33 cm animal research system, Rev. Sci. Instrum. 72 (2001) 4292–4294.
[28] B. Beck, D.H. Plant, S.C. Grant, P.E. Thelwall, X. Silver, T.H. Mareci, H. Benveniste, M. Smith, C. Collins, S. Crozier, S.J. Blackband, Progress in high field MRI at the University of Florida, Magn. Reson. Mater. Phys. Biol. Med. 13 (2002) 152–157.
[29] D.M. Ginsberg, M.J. Melchner, Optimum Geometry of saddle shaped coils for generating a uniform magnetic field, Rev. Sci. Instrum. 41 (1970) 122–123.
[30] X. Zhang, A.G. Webb, Design of a transmit-receive phased array probe for MR microscopy, in: 44th Experimental NMR Conference, Savannah, 2003.
[31] E.G. Larsson, D. Erdogmus, R. Yan, J.C. Principe, J.R. Fitzsimmons, SNR-optimality of sum-of-squares reconstruction for phased-array magnetic resonance imaging, J. Magn. Reson. 163 (2003) 121–123.